Chinese Chemical Letters 32 (2021) 2203–2206

Contents lists available at ScienceDirect

Chinese Chemical Letters

journal homepage: www.elsevier.com/locate/cclet

Communication

Accelerating C_{2+} alcohols synthesis from syngas by simultaneous optimizations of CO dissociation and chain growth over CuCo alloy catalyst

Meiling Shui[a], Chao Huang[a], Peiyu Ma[a], Wenjie Li[a], Qun He[a], Wenlong Wu[b], Yisheng Tan[c], Jun Bao[a,*]

[a] National Synchrotron Radiation Laboratory, University of Science and Technology of China, Hefei 230029, China
[b] Hefei National Laboratory for Physical Sciences at the Microscale, Key Laboratory of Strongly-Coupled Quantum Matter Physics of Chinese Academy of Sciences, Key Laboratory of Surface and Interface Chemistry and Energy Catalysis of Anhui Higher Education Institutes, Department of Chemical Physics, University of Science and Technology of China, Hefei 230026, China
[c] State Key Laboratory of Coal Conversion, Institute of Coal Chemistry, Chinese Academy of Sciences, Taiyuan 030001, China

ARTICLE INFO

Article history:
Received 13 September 2020
Received in revised form 12 November 2020
Accepted 8 December 2020
Available online 16 December 2020

Keywords:
CuCo alloy
Syngas
C_{2+} alcohols
CO activation
Synergistic effect

ABSTRACT

With regard to the reaction of higher alcohol synthesis (HAS), the optimizations of activity and selectivity towards C_{2+} alcohol are restricted by the improper equilibrium in two different CO activation pathways and chain growth capacity. Herein, we find that delibrately controlling the compositions of catalysts is an effective strategy to achieve the equilibrium of CO activation pathways and promote the chain growth. As a result, the optimized $Cu_{0.25}Co_{0.75}$ alloy catalyst can achieve a large proportion of higher alcohol in alcohol products ($C_{2+}OH$/MeOH = 4.40), together with high CO conversion of 71.27% and space-time-yield of 147.65 g kg^{-1} h^{-1}. The mechanistic studies suggest that the good performance of $Cu_{0.25}Co_{0.75}$ catalyst is attributed to the synergistic effect between alloyed Cu and Co.

Higher alcohols (C_{2+} alcohols) have attracted worldwide interest by virtue of their promising applications in transportation fuels, gasoline additives and chemical intermediates. Generally, higher alcohols are produced from the hydration of corresponding petroleum-derived alkenes [1–3]. However, the scarcity of petroleum resource impedes the sustainable production of higher alcohols in the future. It is highly desirable to develop an alternative pathway to yield higher alcohols [4–6]. In this regard, catalyzing the syngas derived from coal, natural gas, or renewable biomass gas into higher alcohols is regarded as a promising pathway. Nevertheless, the formation of some by-products, such as methanol and hydrocarbons, is inevitable [7,8]. It is considered that the higher alcohols is generally formed *via* the CO insertion mechanism, in which the adsorbed CO would be dissociated to form methylene species ($-CH_2-$), followed by the growth of alkyl groups [9–11].

Generally, the CuCo alloy catalyst is considered as one of the most active non-noble metal-based catalysts for higher alcohol synthesis (HAS) reaction [12]. It is well established that Cu is responsible for the non-dissociative adsorption and insertion of CO, while Co works as the active site for CO dissociation and chain growth [12]. What is more, it is thought that high dispersion and intimate contact of metals could boost their synergetic process, thereby favoring the formation of C_{2+} alcohols [13,14]. For example, the palygorskite supported Cu-Fe-Co catalyst could exhibit the high conversion of CO (69.1%), while the proportion of higher alcohols in alcohol products was only 57.5% [13]. The Mn-Al oxide supported CuCo alloy catalyst (3Cu-5Co/(Mn-Al)) could exhibit the highest catalytic performance with a CO conversion of 33.4% and C_{2+} alcohols selectivity towards total alcohols of 57.3% [14]. However, the previously reported bare CuCo catalysts could only achieve the low selectivity towards C_{2+} alcohols.

In this work, we have synthesized CuCo catalysts by the co-reduction method. The Cu/Co ratios of catalysts were deliberately adjusted. As a result, the optimized $Cu_{0.25}Co_{0.75}$ catalyst has exhibited the superior HAS activity with high space-time-yield (STY) of total alcohol (147.65 g kg^{-1} h^{-1}). In particular, the proportion of $C_{2+}OH$ products was 81.5% compared to the total alcohols. The structures of catalysts were characterized by means of advanced techniques and the structure-performance relationship was discussed.

The CuCo precursor was prepared *via* a wet-chemistry reduction method, and the final CuCo alloy samples were obtained

* Corresponding author.
E-mail address: baoj@ustc.edu.cn (J. Bao).

https://doi.org/10.1016/j.cclet.2020.12.022

from the activation of precursors at 300 °C for 4 h in H_2 atmosphere. All of the obtained samples exhibited the consistent X-ray diffraction (XRD) patterns similar to CuCo alloy (PDF# 50-1452, Fig. S1 in Supporting information). Obviously, activation treatment has improved the crystallinity of CuCo. The morphology of CuCo catalysts with different Cu/Co ratios were observed by scanning electron microscopy (SEM). As shown in Fig. S2 (Supporting information), all the CuCo particles show the stacked structure. Furthermore, transmission electron microscopy (TEM) observation shows these particles consist of fine particles with size less than 10 nm (Fig. 1A). High-resolution TEM (HRTEM) image of $Cu_{0.25}Co_{0.75}$ catalyst shows the lattice parameter of 0.208 nm, which corresponds to the (110) plane of the face-centered-cubic (fcc) CuCo alloy (Fig. 1B). The elemental mapping analysis demonstrates the homogeneous distribution of Cu and Co in the entire sample (Fig. S3 in Supporting information). The consistent line scan intensity further confirm the CuCo alloy structure and no obvious phase segregation occurs (Fig. 1C) [15]. The actual ratios of Cu/Co in the prepared samples are evaluated by inductively coupled plasma-atomic emission spectrometry (ICP-AES, Table S1 in Supporting information).

Taking $Cu_{0.25}Co_{0.75}$ as an example, its fine structure was further analyzed *via* the X-ray absorption fine structure spectroscopy (XAFS). In Fig. 1D, the absorption edge at Co K edge of $Cu_{0.25}Co_{0.75}$ is close to that of Co foil (7709 eV), which indicates the metallic states of Co in $Cu_{0.25}Co_{0.75}$. This conclusion can be further confirmed by the similar oscillation curves between $Cu_{0.25}Co_{0.75}$ and Co foil (Fig. S4A in Supporting information). The Fourier-transformed extended XAFS (EXAFS) spectrum of $Cu_{0.25}Co_{0.75}$ just shows one peak at ~2.2 Å, which corresponds to the Co-Co/Cu bonds in $Cu_{0.25}Co_{0.75}$ (Fig. 1E). No peaks related to the bonds between Co and nonmetals can be probed, further demonstrating the metallic phase of $Cu_{0.25}Co_{0.75}$. Similar results are also observed at the Cu K-edge of $Cu_{0.25}Co_{0.75}$ (Figs. 1F and G, Fig. S4B in Supporting information).

To obtain the surface information of samples, X-ray photoelectron spectroscopy (XPS) was performed. The survey profile shows the coexistence of Cu and Co in the sample (Fig. S5 in Supporting information). High-resolution XPS spectra of Co 2p in Fig. 1H shows two prominent peaks at ~802 eV and ~797 eV, which are assigned to the Co^{2+} $2p_{1/2}$ and Co^0 $2p_{1/2}$, respectively. The peaks at ~781 eV and ~778 eV should be assigned to the Co^{2+} $2p_{3/2}$ and Co^0 $2p_{3/2}$, respectively. For Cu 2p XPS spectra of samples, the binding energies at ~952 eV and ~932 eV should correspond to the $Cu^{0/+}$ $2p_{1/2}$ and $2p_{3/2}$, respectively (Fig. 1I). To distinguish the Cu^0 and Cu^+, the Cu Auger LMM analysis was carried out. It can be seen that the Cu^0 is prominent, together with less Cu^+ (Fig. 1J). The calculated Cu/Co ratios according to the XPS results were listed in Table S2 (Supporting information).

The catalytic HAS performances of the as-prepared CuCo catalysts were evaluated in a fixed-bed reactor under 3.0 MPa of syngas (60 vol% H_2, 30 vol% CO and 10 vol% N_2) with gas hourly space velocity (GHSV) of 3900 h^{-1}. Table 1 shows the effect of the reaction temperature on the catalytic performances. The CO conversion and total alcohol STY could achieve the maximum values at 250 °C. The further increasing of the reaction temperature could result in the production decrease of alcohols. In this work, the appropriate reaction temperature (250 °C) could achieve the balance bewteen reaction rate and thermodynamics. Finally, the optimal performance can be obtained. Both CO

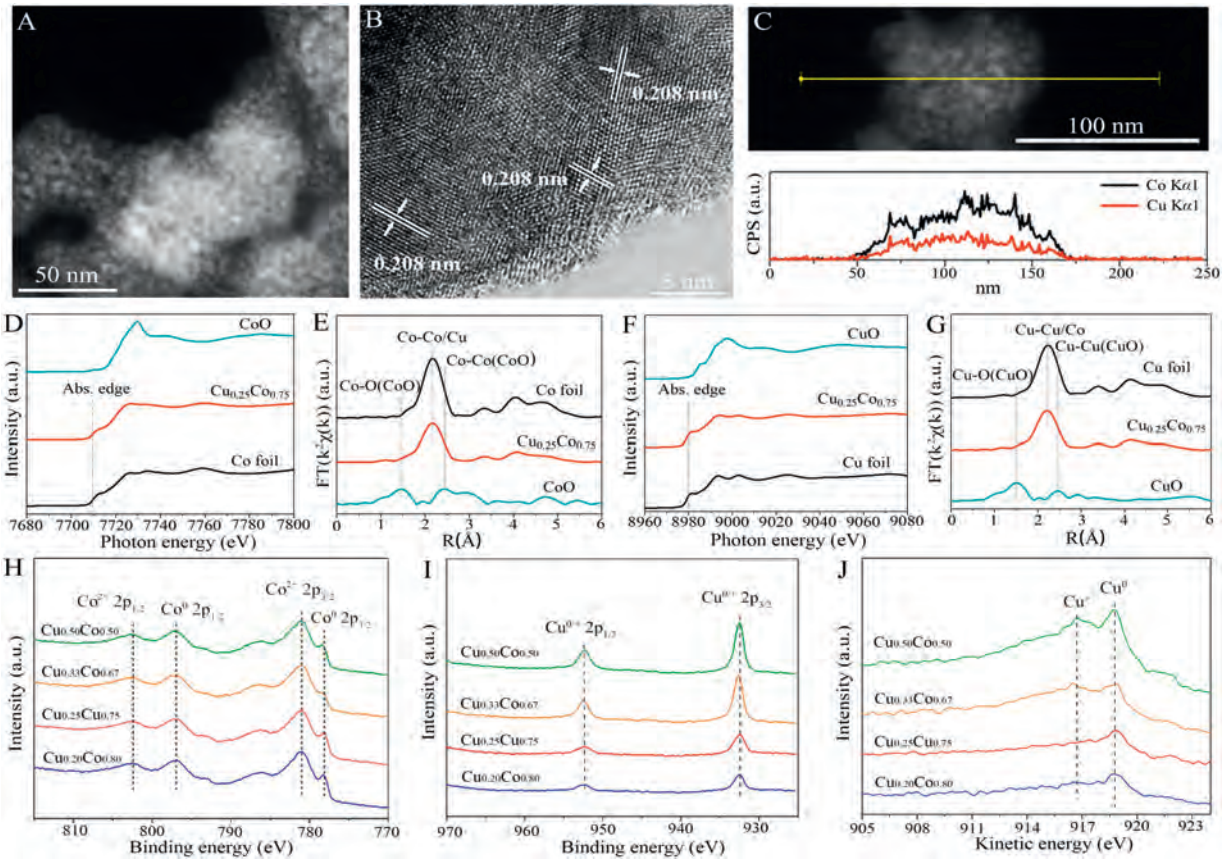

Fig. 1. (A) TEM, (B) HRTEM, and (C) line-scan profile of $Cu_{0.25}Co_{0.75}$ catalyst. (D) Co K-edge XAFS and (E) EXAFS spectra of $Cu_{0.25}Co_{0.75}$. (F) Cu K-edge XAFS and (G) EXAFS spectra of $Cu_{0.25}Co_{0.75}$. High-resolution XPS of (H) Co 2p and (I) Cu 2p and (J) Cu Auger LMM spectra of CuCo alloy catalysts.

Table 1
Effect of reaction temperature on the catalytic performance of $Cu_{0.25}Co_{0.75}$ catalyst.[a,b]

Temperature (°C)	CO Conv. (%)	Alc. STY (g kg^{-1} h^{-1})
230	51.57	120.90
250	71.27	147.65
270	69.23	101.83

[a] Reaction condition: 0.5 g catalyst, T = 250 °C, P = 3.0 MPa, GHSV = 3900 h^{-1}, H_2/CO = 2.
[b] Conv. = conversion, Alc. STY. = space-time-yield of alcohols.

conversion and alcohol selectivity are calculated based on a CO_2-free basis.

The effect of Cu/Co ratios on the HAS performance is shown in Table 2. The catalytic behaviors show a volcano-shaped function for the ratios. Obviously, the $Cu_{0.25}Co_{0.75}$ catalyst has exhibited the best performance for HAS. Regarding $Cu_{0.25}Co_{0.75}$ catalyst, the STY of total alcohols reaches up to 147.65 g kg^{-1} h^{-1} with a CO conversion of 71.27% under the mild conditions of 3.0 MPa, 250 °C and 3900 h^{-1}. The distributions of alcohol products over catalysts with different Cu/Co ratios are presented in Fig. 2. It can be seen that the $Cu_{0.25}Co_{0.75}$ catalyst has achieved the highest C_{2+}OH/MeOH ratio of 4.40. These results suggest that the dissociation adsorption of CO over Co species plays an important role in the synthesis of higher alcohols.

The catalytic performances of some representative catalysts reported are listed in Table S3 (Supporting information). Taking activity and selectivity into considerations, CuCo alloy catalysts prepared in our work show much better catalytic performance in terms of the conversion of CO and the selectivity towards C_{2+} alcohols.

The temperature programmed reduction (TPR) experiments of precursors in H_2 atmosphere (H_2-TPR) were carried out to explore the reduction information. As shown in Fig. 3A, the peak between 140 °C and 220 °C is due to the reduction of CuO_x to Cu. It is obvious that the peak intensity of CuO_x-to-Cu reduction strengthens with the increase of Cu amount. These results are also consistent with the XPS and Auger analyses above. The peaks locate at 220−550 °C region should be attributed to the reduction of CoO_x to Co [15]. It is worth noting that the $Cu_{0.25}Co_{0.75}$ catalyst has achieved the lowest reduction temperature among them. This should be attributed to the interaction between Cu and Co by forming CuCo alloy phase. The formed metallic structure of CuCo alloy has also been confirmed by the XAFS resluts (Figs. 1D–G). The CuCo alloy structure was proved to be the catalytic active sites in HAS [3].

The normalized temperature programmed desorption (TPD) curves in CO atmosphere (CO-TPD) of the pure Cu and pure Co catalysts are shown in Fig. S6 (Supporting information). For pure Cu, the desorption temperature of CO is less than 410 °C; while pure Co exhibited a higher desorption temperature of CO more than 500 °C. TPD curve of the H_2-reduced catalysts in He without

Table 2
CO hydrogenation over the catalysts as a function of Cu/Co ratios.[a,b]

Catalysts	CO Conv. (%)	C_{2+}/MeOH	Alc. STY (g kg^{-1} h^{-1})
$Cu_{0.50}Co_{0.50}$	41.02	2.14	85.54
$Cu_{0.33}Co_{0.67}$	58.84	3.28	114.82
$Cu_{0.25}Co_{0.75}$	71.27	4.40	147.65
$Cu_{0.20}Co_{0.80}$	62.24	3.93	123.08

[a] Reaction conditions: 0.5 g catalyst, T = 250 °C, P = 3.0 MPa, GHSV = 3900 h^{-1}, H_2/CO = 2.
[b] Conv. = conversion, Alc. STY. = space-time-yield of alcohols. Both CO conversion and alcohol selectivity are calculated based on a CO_2-free basis. C_{2+}OH/MeOH is based on the moles of carbon.

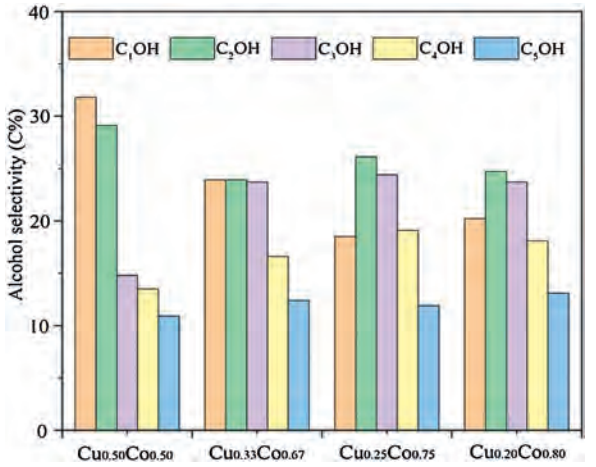

Fig. 2. The distribution of alcohol products over the catalysts with different Cu/Co ratios.

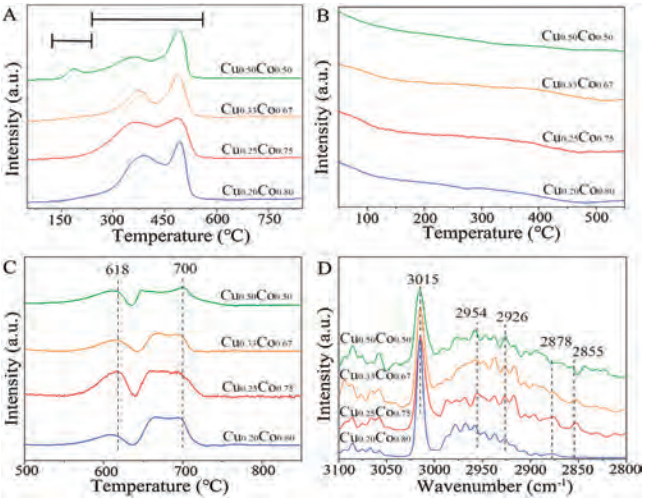

Fig. 3. TPR profiles of H_2 (A), TPD profiles of CO with temperature of 50-550 °C (B), 500-850 °C (C), and *in-situ* DRIFTS spectra (D) for CuCo catalysts with varying molar ratios of Cu/Co.

CO pre-adsorption showed no obvious desorption (Fig. S7 in Supporting information). CO-TPD curves with different Cu/Co ratios are shown in Figs. 3B and C. The low-temperature peaks of the catalysts at about 50−500 °C are attributed to the desorption of CO over Cu species (Fig. 3B), and the high-temperature peaks at more than 500 °C can be ascribed to the dissociation of the adsorbed CO over Co species (Fig. 3C). When the ratios of Cu/Co increase, the desorbed peak areas of CO-species over Cu species are barely changed, and the slight adsorption of CO occurs on all catalysts. The observed desorption peaks at high temperature indicates that the strong CO adsorption mainly occurs on the Co sites which should contribute to the dissociative adsorption of CO. Obviously, by adjusting the amounts of Cu in catalyst, the $Cu_{0.25}Co_{0.75}$ catalyst finally exhibits the largest desorption peak area, which implies the non-dissociative adsorption of more CO on $Cu_{0.25}Co_{0.75}$ catalyst. It is agreed with the obtained highest C_{2+}OH/MeOH ratio for $Cu_{0.25}Co_{0.75}$ catalyst. In a word, the adsorption of CO over catalysts can be adjusted by regulating the Cu/Co ratios in HAS, thereby controlling the overall catalytic performance [16–18].

To investigate the average carbon chain length and carbon chain growth capacity of hydrocarbon molecules produced, *in-situ*

DRIFTS analyses were performed. As shown in Fig. 3D, the peak at 3015 cm^{-1} should be related to the formation of gaseous methane (CH_4), and the peaks at 2954 cm^{-1} and 2926 cm^{-1} should represent the asymmetric CH stretching vibration of the methyl species ($-CH_3$) and methylene species ($-CH_2-$), respectively. The peak at 2878 cm^{-1} should be attributed to the symmetric CH stretching vibration of the methyl species ($-CH_3$), and the peak at 2855 cm^{-1} shoud be assigned to the symmetric CH stretching vibration of methylene species ($-CH_2-$). The representative peak area of $-CH_2-$ species locates at 2925–2930 cm^{-1}, which signifies the asymmetric extension of $-CH_2-$ species. The peak area of $-CH_3$ species is at 2955–2960 cm^{-1}, which represents the asymmetric extension of $-CH_3$ species. The following formula is used to calculate the growth capacity of the carbon chain (Eq. 1):

$$\text{Carbon chain growth} = \frac{\text{Area}(-CH_2- \text{ species})}{\text{Area}(-CH_3 \text{ species})} \quad (1)$$

The calculated peak area ratios are shown in Table S4. Obviously, $Cu_{0.25}Co_{0.75}$ catalyst has achieved the highest peak area ratio of $(-CH_2-)/(-CH_3)$ of 0.8226. The CH_2 group can be coupled with the dissociative species of CO to increase the length of the carbon chain. The above results indicate that the growth ability of carbon chain is strongest over $Cu_{0.25}Co_{0.75}$ catalyst [19–21]. Finally, the fine structures of spent $Cu_{0.25}Co_{0.75}$ catalyst were explored by XAFS. As can be seen in Fig. S8 (Supporting information), there are no obvious changes of absorption edge and peaks for fresh and spent $Cu_{0.25}Co_{0.75}$, suggesting the preservation of the robust CuCo alloy structure even after reaction.

In summary, we have successfully developed the CuCo catalysts with varying Cu/Co ratios. As experimentally analyzed, the $Cu_{0.25}Co_{0.75}$ catalyst with Cu/Co molar ratio of 0.30 has achieved the simultaneous optimization of activity and selectivity towards higher alcohols synthesis in HAS. Based on mechanistic studies, the high activity of $Cu_{0.25}Co_{0.75}$ catalyst should be attributed to the strong dissociation adsorption of CO and the strong carbon chain growth ability. This work highlighted a promising strategy to design active and selective catalysts for HAS.

Declaration of competing interest

The authors declare that they have no known competing financial interests or personal relationships that could have appeared to influence the work reported in this paper.

Acknowledgments

This work was supported by National Key Research and Development Program of China (Nos. 2017YFA0403402, 2019YFA0405602), National Natural Science Foundation of China (Nos. 21673214, U1732272) and Foundation of State Key Laboratory of Coal Conversion (No. J20-21-902).

Appendix A. Supplementary data

Supplementary material related to this article can be found, in the online version, at doi:https://doi.org/10.1016/j.cclet.2020.12.022.

References

[1] H.T. Luk, C. Mondelli, D.C. Ferré, et al., Chem. Soc. Rev. 46 (2017) 1358–1426.
[2] J. Bao, G. Yang, Y. Yonyama, et al., ACS Catal. 9 (2009) 3026–3053.
[3] A. Cao, G. Liu, L. Wang, et al., J. Mater. Sci. 51 (2016) 5216–5231.
[4] M. Ghashghaee, S. Sadjadi, S. Shirvani, et al., Catal. Lett. 147 (2017) 318–327.
[5] S. Li, H. Guo, C. Luo, et al., Catal. Lett. 143 (2013) 345–355.
[6] J. Anton, H. Ruland, S. Kaluza, et al., Catal. Lett. 145 (2015) 1374–1381.
[7] Y. Xiang, R. Barbosa, N. Kruse, ACS Catal. 4 (2014) 2792–2800.
[8] H. Guo, S. Li, F. Peng, et al., Catal Lett. 45 (2015) 620–630.
[9] J. Su, Z. Zhang, D. Fu, et al., J. Catal. 336 (2015) 94–106.
[10] Z. Zhao, W. Lu, R. Yang, et al., ACS Catal. 8 (2017) 228–241.
[11] Z. Wang, N. Kumar, J. Spivey, J. Catal. 33 (2016) 1–8.
[12] T. Lin, X. Qi, X. Wang, et al., Angew. Chem. Int. Ed. 58 (2019) 4675–4679.
[13] H. Guo, H. Zhang, F. Peng, et al., Appl. Clay Sci. 111 (2015) 83–89.
[14] L. Zhao, J. Duan, Q. Zhang, et al., Ind. Eng. Chem. Res. 57 (2018) 14957–14966.
[15] Y. Cen, S. Zhu, J. Guo, et al., RSC Adv. 8 (2018) 9152–9160.
[16] L. Shi, W. Chu, S. Deng, J. Nat. Gas Chem. 20 (2011) 8–52.
[17] Y. Cheng, J. Lin, K. Xu, et al., ACS Catal. 6 (2016) 389–399.
[18] J. Huang, W. Qian, H. Zhang, et al., Catal. Sci. Technol. 7 (2017) 5530–5796.
[19] W. Qian, H. Wang, Y. Xu, et al., Ind. Eng. Chem. Res. 58 (2019) 6288–6297.
[20] W.M. Hexana, N.J. Coville, App. Catal. A: Gen. 377 (2010) 150–157.
[21] Y. Xiang, R. Barbosa, N. Kruse, et al., ACS Catal. 4 (2014) 2792–2800.